# The mechanism of decomposition of serpentines from peridotites on heating

Nshan Zulumyan · Andrei Mirgorodski ·
Anna Isahakyan · Hayk Beglaryan

**Abstract** Serpentines from peridotites of San Jose and New Idria (California, USA) were previously heat treated ranging from 400 to 1,260 °C, and then leached by using an original approach for acid processing of dehydrated serpentines. This approach is capable of releasing from the dehydrated serpentines ortho-$[SiO_4]^{4-}$, di-$[Si_2O_7]^{6-}$, and other silicate anions, and moving them into solution in the form of soluble silicic acids. The discovery of these anions has led to the idea of the existence of differences in electronic configuration of Si–O bonds in siloxane bridges and different amount and allocation of ortho-$[SiO_4]^{4-}$ and meta- $[(SiO_3)^{2-}]_n$ silicate anions in serpentines silicate layers thus providing a new deeper insight into the mechanism of the temperature-induced decomposition of the serpentine silicate structure. It should be emphasized that in spite of a great number of studies devoted to the temperature-induced dehydroxylation and recrystallization processes of serpentine minerals, the mechanism of serpentine decomposition is still poorly understood because no one has studied particularities of the structural organization of silicate layers in serpentines. The effect of thermal treatment at different temperatures ranging from 400 to 1,260 °C for 2 h on the above mentioned serpentinite samples was characterized by thermal analysis, X-ray diffraction, and chemical analysis. The observed evidence made possible a comprehensive modeling of the relevant dehydroxylation, high-temperature crystallization, and recrystallization reactions. Complemented by chemical analysis data, the results obtained allows understanding the basic principles of the serpentine decomposition and crystallization processes, which govern the formation of stable high-temperature products like forsterite, enstatite, and protoenstatite, as well as the formation of different amount of silicic acids in solution via the new approach. These studies are of great interest and value to the pure and applied material sciences connected with serpentinites.

**Keywords** Serpentine · Dehydroxylation · Decomposition · Si–O(Si) bonds · Silicate anions

N. Zulumyan (✉) · A. Isahakyan · H. Beglaryan
The Institute of General and Inorganic Chemistry of the National Academy of Sciences of the Republic of Armenia (IGIC NAS RA), Argutyan str. 10, lane 2, 0051 Yerevan, Armenia
e-mail: zulumnshan@rambler.ru

A. Mirgorodski
Laboratoire Science des Procedes Ceramiques et de Traitements de Surface, UMR 7315 CNRS, Centre Europeen de la Ceramique, 12 rue Atlantis, 87068 Limoges Cedex, France

## Introduction

Silicate rock-forming minerals constitute the major part (about 90 %) of the Earth's crust, thus representing a raw material stock for modern and future human civilizations. In particular, serpentine minerals $(Mg, Fe)_3Si_2O_5(OH)_4$ are promising for the high-yield synthesis of magnesium-containing compounds, as well as of silica [1–7]. Of special interest are their temperature-induced transformations which carry certain information important for different fields of science and for finding cost effective ways of serpentinites processing [8–32].

The serpentine minerals belong to phyllosilicate group (layer-type silicates or sheet silicates). They are formed by alteration (hydration) of magnesium-rich silicate

minerals (e.g., olivine $(Mg, Fe)_2SiO_4$) and appear in mafic and ultramafic rocks.[1] They have layer structures built of 1:1 alternately stacked tetrahedral and octahedral sheets. The tetrahedral sheets, representing the complex silicate anions, can be regarded as resulting from the two-dimensional polymerization of Si-centered tetrahedra sharing three oxygen atoms with neighboring tetrahedra. The unshared oxygen atoms are bonded to Mg atoms which jointly with OH units form the octahedral sheets. There are three widely-spread natural polymorphs of serpentine, chrisotile, lizardite, and antigorite, whose important natural deposits are of universal occurrence (USA, Canada, Italy, Russia, Paraguay, Armenia, New Zealand, and so on).

Thermal behavior of serpentine group minerals has been widely studied in the past and it has been generally established the following statements. The heat treatment of serpentinites within the temperature range of 550–800 °C gives rise to two simultaneous processes: (i) that removing constitutional (hydroxyl) water, and (ii) that distracting crystalline structure [8–16]. Universally, the relevant DTA curves have different minima manifesting strong endothermic behavior [16–30]. As a rule, it is accompanied by the sharp mass loss of the rock, and is followed by noticeable exothermic effect (ending at about 850 °C) caused by the forsterite $(Mg_2SiO_4)$ and partly by clinoenstatite $(Mg_2Si_2O_6)$ formations from the serpentine mass becoming amorphous [17–30]. Subsequent heating up to the 1,000 °C results in the recrystallization of the previously formed forsterite and the formation of clinoenstatite crystals [18, 29, 31]. Much lower exothermic peak intensity sometimes observable within the temperature range of 1,160–1,260 °C is attributed to the beginning and the end of the protoenstatite $(MgSiO_3)$ recrystallization [31].

It should be noted that detailed versions of dehydroxylation and dehydration mechanisms and high-$T$ crystallization for chrysotile and antigorite are reported in many studies, whereas the temperature-induced processes of lizardite have been the subject of a few articles. One of our goals lies in trying to improve this situation: our study is devoted to the study of lizardite.

Notwithstanding a great body of studies devoted to the temperature-induced dehydroxylation and recrystallization processes of serpentine minerals in air at ambient pressure, no final clarity is presently researched in this field. In particular, the questions: *What is the manner in which the organization of silicate layers in serpentine minerals has an impact on the stability of amorphous dehydroxylated phases and the decomposition extent of serpentine structure? How does it influence the process of forsterite and enstatite formation?* remain the open questions. The body of our researches is aimed at finding answers to these questions.

Recently, a new approach to the acid processing of dehydrated serpentine minerals in question has been developed capable of moving silicic acids into solution [1], thus offering new possibilities for a deeper insight into the perception of serpentine silicate layer decomposition on heating. In particular, it has been first found that the dehydroxylation and the global amorphization of the serpentine crystalline structure are simultaneously accompanied by the partition of 2D-serpentine silicate layer (SSL) and releasing of silicate anions of various complexities, being in major part the orthosilicate ones [32]. It should be noted that the previous methods available for acid processing of serpentinites do not allow of discovering the formation of soluble silicic acids [2–5].

Using this approach, the studies of several samples of antigorite taken from Armenian deposits, originating from different parents rocks (apodunites, apoperidotites, and peroxynites) were conducted [31, 32]. It has been experimentally established that the SSL integrity and the amount of silicic acids moved into solution via the acid processing of the heated serpentinite samples directly depend on their genetics. Moreover, the discovery of different amount of silicic acids in the solution has revealed challenging particularities in the electronic structure of Si–O bonds of the SSL siloxane bridges [31–35].

In this connection, it can be recalled that the natural serpentine minerals are made owing to a low grade metamorphic alteration of magnesium-rich minerals such as olivine $(Mg, Fe)_2SiO_4$ and pyroxene $(Mg, Fe)_2Si_2O_6$. Their SSL was mainly formed in the serpentine-forming solution under hydrothermal conditions below 500 °C via the polycondensation of the previously formed molecules of *ortho-* $H_4SiO_4$ and *meta-* $(H_2SiO_3)_n$ silicic acids [36]. The following simplified version of the serpentine formation can be proposed:

$$Mg_2SiO_4 + MgSiO_3 + 6H_2O \xrightarrow{CO_2,\ T,\ P} 3Mg(OH)_2 + H_4SiO_4$$
$$+ H_2SiO_3 \rightarrow (Mg)_3Si_2O_5(OH)_4 + 4H_2O$$
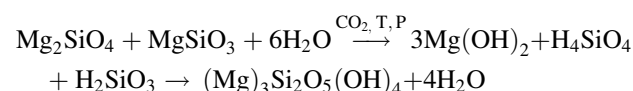
Naturally, the Si–O(Si) bonds of siloxane bridges made up under such conditions are weaker and therefore splittable with comparative ease upon thermal and mechanical influences than the Si–O(Si) ones of *meta*-silicate chains $[(SiO_3)^{2-}]_n$ formed in magma under high pressure at temperature over 1,000 °C [32–35].

This fact appears worthy of the further comments. Actually, silicate anions ($[SiO_4]^{4-}$, $[Si_2O_7]^{6-}$ etc., and $[(SiO_3)^{2-}]_n$) moved into serpentine-forming solution (see

---

[1] Mafic rocks have around 50 % or less (55–45 %) silica and a lot of magnesium and iron; and ultramafic ones contain silica less than 45 %, generally more than 18 % MgO.

above) originate from the parent ultramafic rocks that are dunites,[2] peridotites,[3] and pyroxenites.[4] In turn, these rocks can consist either of the completely formed individual units of olivine and pyroxene crystals or of the mixed and bonded anion groups like alligation. It has been evidenced that the processes which cause the considered anions to move into serpentine-forming solution, and to make up the SSL depend on the two factors: (a) on the variety of parent ultra-mafic rocks and (b) on their anion states prior to serpentinization. The central point is that the relevant experiments have shown that serpentine specimens having the same crystal structure, but originated from different parent rocks manifest some differences when being exposed to thermal, mechanical, and chemical effects [31, 32]. Consequently it has been concluded that the factors (a) and (b) play an important role in the structural organization of such anions in the SSL, thus predetermining their fundamental physical and chemical properties.

Evidently, to deeper understand their nature and to verify the universal character of the results mentioned above, the geography of the samples under study should be necessarily widened, i.e., the samples from deposits other than Armenian ones must be subjected to the analogous investigations. In the present study, we wished to study in detail the specific properties of the silicate layers of serpentinites samples located in San Jose and New Idria (California, USA) [37, 38] by undergoing physicochemical investigations, involving the DTA, X-ray phase study, and chemical analysis data, and to prove that the mechanism of serpentines decomposition does not depend on their polymorph, and is mainly correlated with the allocation and proportion of hydrated *ortho*- and *meta*-silicate anions originally involved in the process of the silicate layer formation from the parent ultramafic rocks.

To our belief such a study could clarify the molecular mechanisms of hydrothermal processes which occurred in ultramafic rocks, and reveal the microscopic structural factors driving the serpentinite decomposition upon various thermodynamical and chemical influences thus adding to the geologic and mineralogical knowledge of serpentine minerals. In such a way, the systematic fundamental knowledge can be obtained necessary to predict the amount of synthesized soluble silicic acids, magnesium- and iron-related compounds, and other products representing

interest for the pure and applied material sciences, as well as for the engineering and technology.

## Experimental

The main subjects of our study were the samples of serpentinites formed from peridotites and located in San Jose (the samples of SJ-1, SJ-2) and New Idria (the sample of NI-1) (California, USA) [38]. The chemical composition of these samples is given in Table 1. Since our interest was focused on the amount of MgO, $SiO_2$, and volatile content of the rocks, the chemical analysis did not attempt to differentiate the other individual metal oxides, and their total amount ($R_2O_3$) is just given.

The mass of test specimens subjected to DTA and X-ray phase analysis was 500 mg and 1,000 mg for chemical analysis.

Dehydroxylation and recrystallization of these samples have been studied in air by DTA from room temperature up to 1,000 °C and by X-ray phase analysis.

DTA and thermogravimetry (TG) measurements were performed in air at a heating rate of 10 °C min$^{-1}$ by using DERIVATOGRAPH Q-1500D equipment produced by the MOM company (Hungary).

X-ray phase analysis data were obtained by XRPD by using Dron-3 diffractometer equipped with nickel filter, under the following conditions: CuKα-radiation; power supply 25 kV/10 mA; and angular range $2\theta = 8°–80°$ at the room temperature in air. All the reflections were identified and interpreted using the ICDD–JCPDS database of crystallographic 2004.

In addition, all the samples (SJ-1, SJ-2, and NI-1) preliminarily grinded and sieved through the sieve 250 holes sm$^{-2}$ to achieve a particle size's distribution of about 0.1–0.2 μm, with a maximum grain size of about 0.25 μm were annealed at the temperatures of 400, 450, 500, 550, 600, 650, 700, 750, 850, 1000, 1160, and 1260 °C within 2 h. After heat treating at a certain temperature, each of the samples was subjected to X-ray phase analysis in order to clear up all the processes occurring on heating. Besides, each of the heated samples was leached by hydrochloric acid during 10 min, and then the formed

---

[2] Dunite is an ultramafic plutonic igneous rock. The mineral assemblage is greater than 90 % olivine (Mg, Fe)$_2$SiO$_4$ with minor amounts of pyroxene (Mg, Fe)$_2$Si$_2$O$_6$ and other minerals (chromite and pyrope).

[3] Peridotite is an ultramafic plutonic igneous rock consisting mostly of olivine (40–90 %) and pyroxene.

[4] Pyroxenite is an ultramafic plutonic igneous rock that consists of dark minerals in the pyroxene group plus a little olivine (10 %).

**Table 1** The chemical composition of the SJ-1, SJ-2, and NI-1 samples. $R_2O_3$ = other individual metal oxides

| Samples | Components and their mass% | | | | SUM | $\frac{\text{Moles MgO}}{\text{Moles SiO}_2}$ |
|---|---|---|---|---|---|---|
| | $SiO_2$ | $R_2O_3$ | MgO | Volatiles | | |
| SJ-1 | 38.58 | 10.93 | 35.72 | 14.50 | 99.73 | 1.38 |
| SJ-2 | 39.38 | 10.06 | 35.97 | 14.76 | 99.67 | 1.36 |
| NI-1 | 37.11 | 13.94 | 34.84 | 13.60 | 99.49 | 1.40 |

sludge was decanted and filtered [1]. 30 mL of the filtrate was separated for quantitative chemical analysis, and unreacted residues which remained after acid processing of the serpentinite samples were annealed at different temperatures and also subjected to X-ray phase analysis.

The quantitative chemical analysis was carried out involving gravimetric, complexometric, and colorimetric methods.

## Results and discussions

The XRPD patterns of the SJ-1, SJ-2, and NI-1 samples point to the predominance of lizardite in these samples (Card No 84–1391); in addition, the SJ-2 sample contains a tangible amount of clinochrysotile(Card No 31–0808), and the others—mainly orthochrysotile (Card No 22–1162) (Fig. 1).

The XRPD patterns for the SJ-1 and SJ-2 specimens heat treated within the temperature ranging from 600 to 1,260 °C are identical, so below the XRPD patterns for the SJ-1 are given.

The water loss values on heating have been estimated from the mass loss curves (TG) of water, and their graphic presentation is shown in Fig. 2. It should be noted that the maximum percentage of water in serpentinites is 14 %.
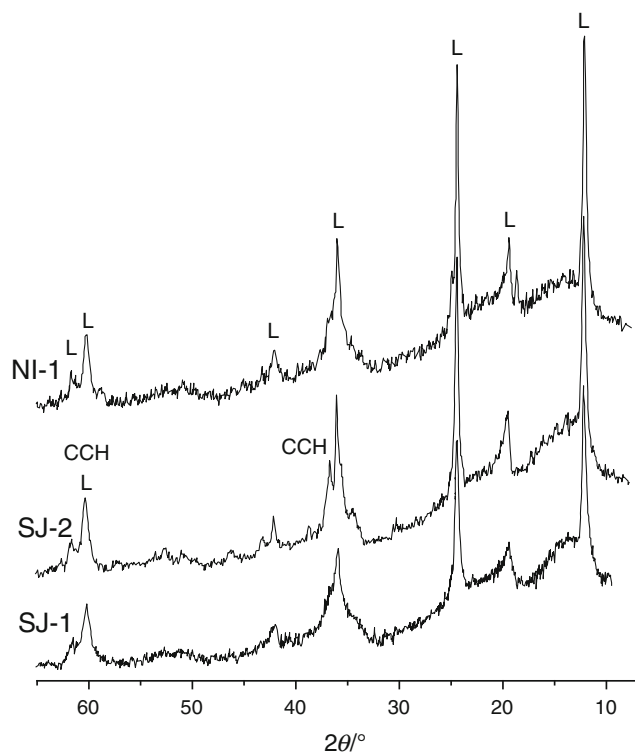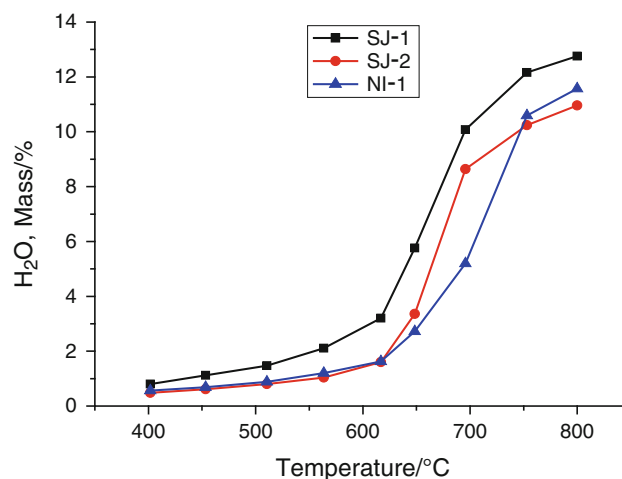


**Fig. 2** The plot of the $H_2O$ loss value for the SJ-I, SJ-2, NI-1 samples versus temperature

The extraction ratio of main components that moved into solution during the acid processing have been calculated and in the same manner graphically represented in terms of their oxides (Fig. 3).

After acid processing of the samples previously heated at the temperature of 400 °C, silicic acids are readily discovered in the solution (Fig. 3). This fact indicates that at such a temperature the process of the destruction already occurs and it is accompanied by the releasing of the simplest silicate anions forming the respective soluble silicic acids. In addition, the slow and smooth trend of curve corresponding to water removal observable on the TG curve (Fig. 4) indicates that the process of the SSL destruction is bound up with the process of hydroxyl water formation even at comparatively low temperatures (∼400 °C). The incomplete minerals destruction and the slow hydroxyl water formation are observed on heating up to the temperature of 600 °C (Figs. 2, 3). Above this temperature, the yields of soluble silicic acids continuously and appreciably increase, and their maxima are obtained for the samples annealed at the temperature of 750 °C (Fig. 3). The chemical analysis shows that the maximal values of soluble silicic acids directly depend upon the maximal amount of hydroxyl water (Figs. 2, 3).

It should be noted that the XRPD patterns for the SJ-1, SJ-2, and NI-1 specimens heat treated within the temperature range from 600 to 850 °C have some distinctive features: for the SJ-1 and SJ-2 samples the forsterite reflections appear at the temperature of 700 °C (Fig. 5), and for the NI-1—at the lower temperature of 650 °C (Fig. 6) (Card No 85–1362). However, there are no diffraction peaks of forsterite in the XRPD patterns of the residues which remain after the acid processing of the samples of SJ-1, SJ-2, and NI-1 annealed up to the temperature of 750 °C (Figs. 7, 8). The X-ray phase analysis data for the residues and the results of chemical



**Fig. 1** The XRPD patterns of the unheated serpentinites samples before the leaching. *L* lizardite, *CCH* clinochrysotile
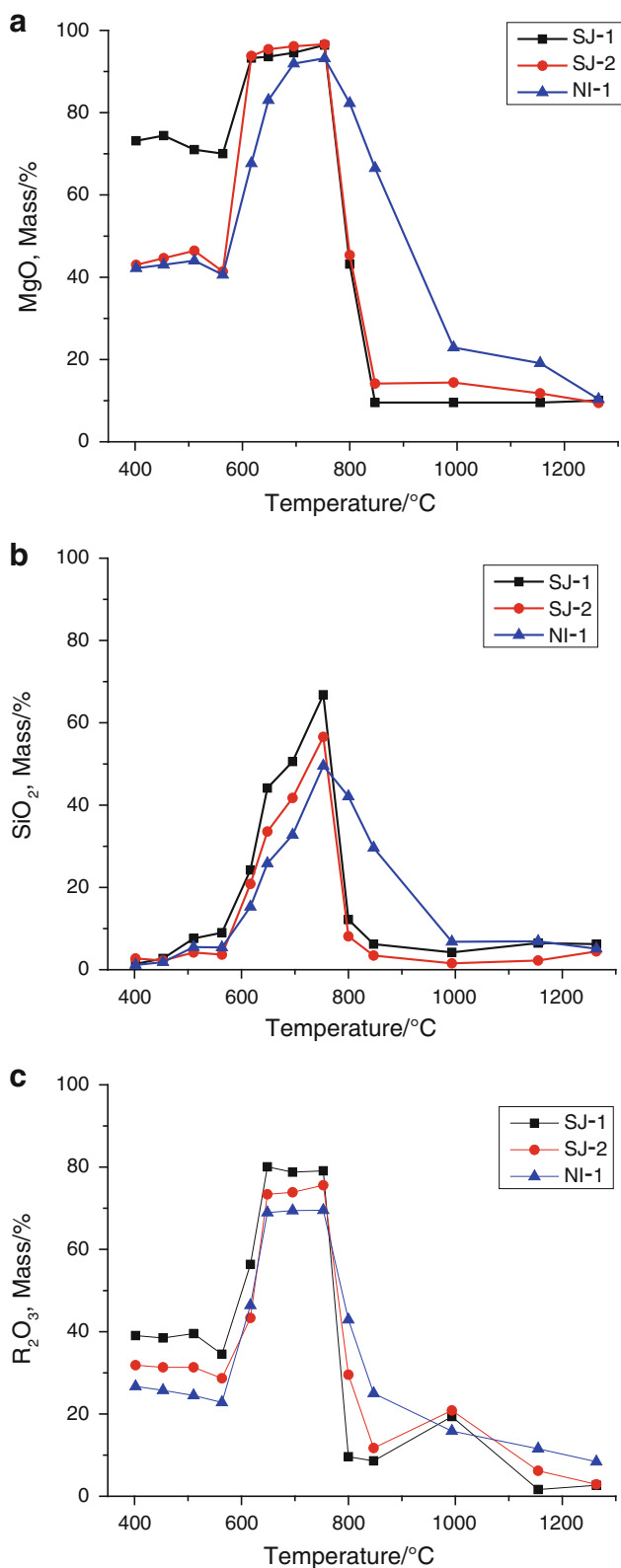
**Fig. 3** The plots of the extraction ratio of main components for the SJ-1 and SJ-2; NI-1 samples versus temperature. **a** MgO, **b** SiO$_2$, **c** R$_2$O$_3$
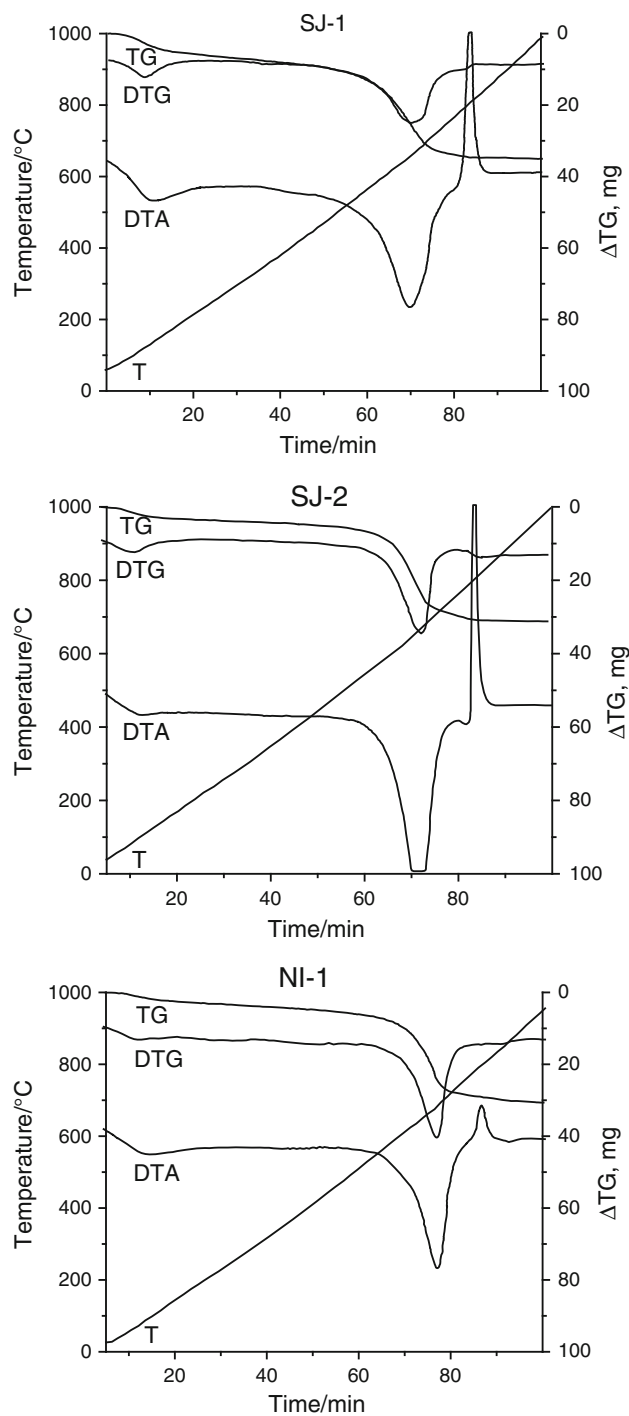


**Fig. 4** Thermal analysis curves for the serpentinite samples. *TG* thermogravimetry, *DTG* derivative thermogravimetry, DTA differential Thermal analysis curve. The *vertical axis* label applies to the DTA curve

analysis of soluble silicic acids (Fig. 3) allow concluding that the forsterite formed on heating up to 750 °C is present in an incompletely formed state and is therefore easily decomposable by diluted acid.
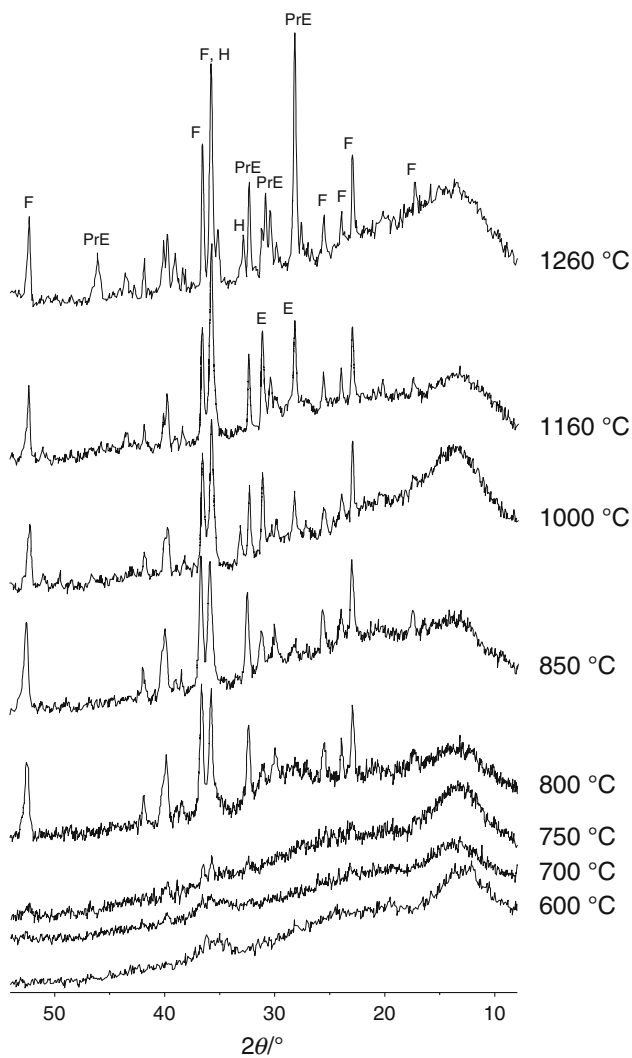
**Fig. 5** The XRPD patterns of the SJ-1 sample after heat treatment. *F* forsterite, *E* enstatite, *PrE* protoenstatite, *H* hematite

Heat treatment above 750 °C does not promote the silicate layer decomposition. Vice versa, the common decrease of the amount of soluble silicic acids is observed (Fig. 3). At the same time, the noticeable differences between the yields of soluble silicic acids are traced for the SJ-1, SJ-2, and NI-1 samples within the interval of 750–850 °C (Fig. 3). The abrupt decrease of the yields of soluble silicic acids is also observed for the samples of SJ-1 and SJ-2 annealed at the temperature of 800 °C, whereas this event is less tangible for the sample NI-1.

In the XRPD patterns for the residues of the SJ-1 and SJ-2 samples, annealed at the same temperatures, the forsterite reflections are fixed (Fig. 7). These data are indicative of the fact that the above mentioned abrupt decrease of the yields of soluble silicic acids (Fig. 3) is caused by the existence of completely formed forsterite crystals, which are not decomposable by diluted acid during the 10 min processing.
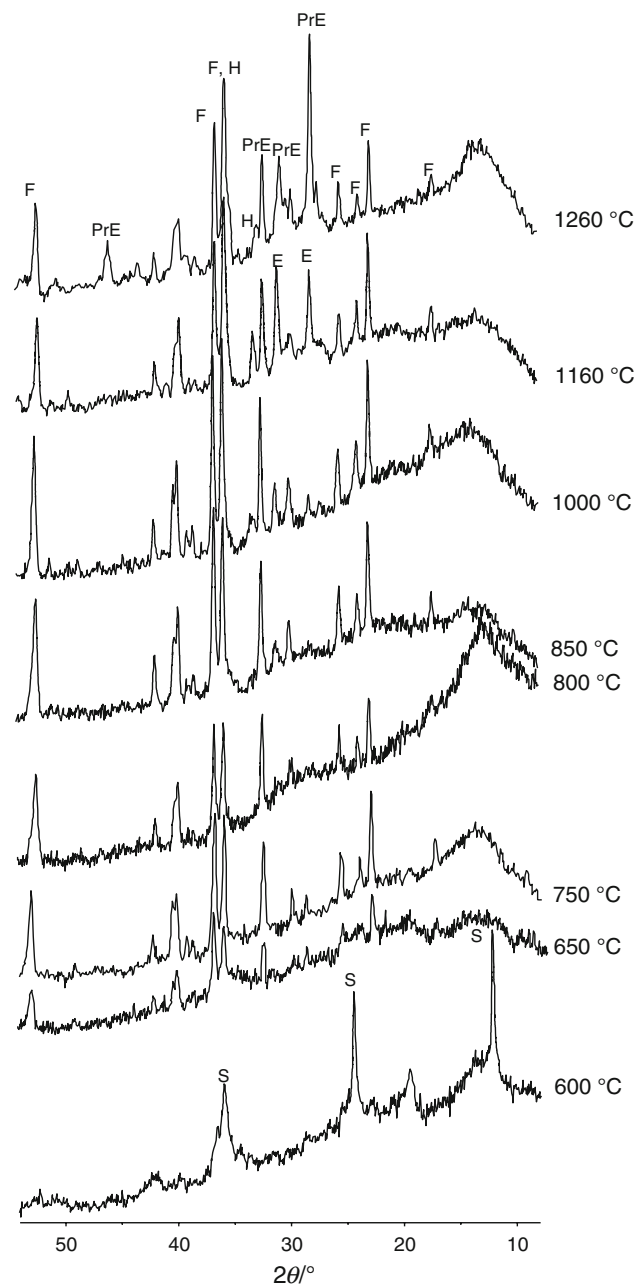


**Fig. 6** The XRPD patterns of the NI-1 sample after heat treatment. *S* serpentine, *F* forsterite, *E* enstatite, *PrE* protoenstatite, *H* hematite

It should be added that the forsterite diffraction peaks of the similar intensity solely appear in the XRPD patterns for the residues of the NI-1 specimen annealed at the temperature of 850 °C (Fig. 8), and the comparatively high yield of soluble silicic acids is observed for it (Fig. 3). So, there is a good reason to think that the forsterite formation is still accompanied by the decomposition of the SSL with releasing of the simplest silicate anions for that sample. The weak reflections of forsterite are hardly traced for the specimen of NI-1 annealed at the temperature of 800 °C (Fig. 8), as a distinct from the forsterite reflections fixed for
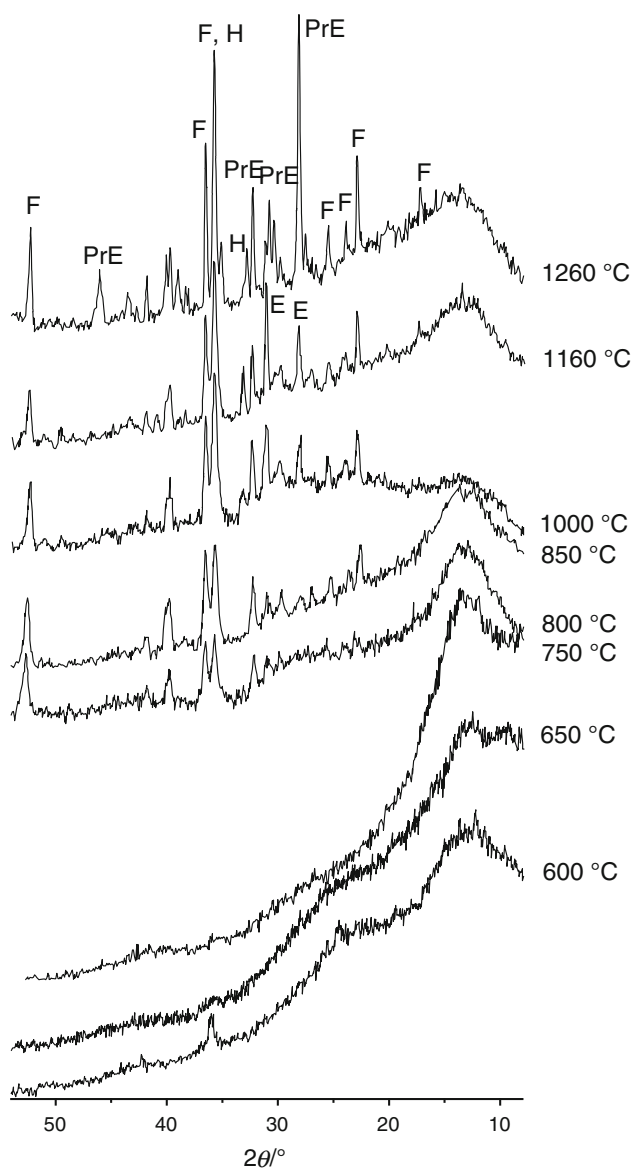
**Fig. 7** The XRPD patterns of the residue remained after acid processing of the SJ-1 sample heat treated at the above mentioned temperatures. *F* forsterite, *E* enstatite, *PrE* protoenstatite, *H* hematite

the SJ-1 and SJ-2 specimens annealed at the same temperature (Fig. 7).

The SJ-1, SJ-2, and NI-1 samples mainly have lizardite crystal structure (Fig. 1) and nearly the same chemical composition (Table 1). Therefore, the certain differences observable for the above samples upon heating can be readily explained by the particularities of silicate layers, i.e., the allocation and distribution of primary *ortho-* and *meta*-silicate anions in the SSL.

The fact that for the sample of NI-1 nano-sized forsterite crystals already get formed at the temperature of 650 °C (Fig. 6) indicates the existence of separate parts mainly consisting of the primary hydrated orthosilicate anions in
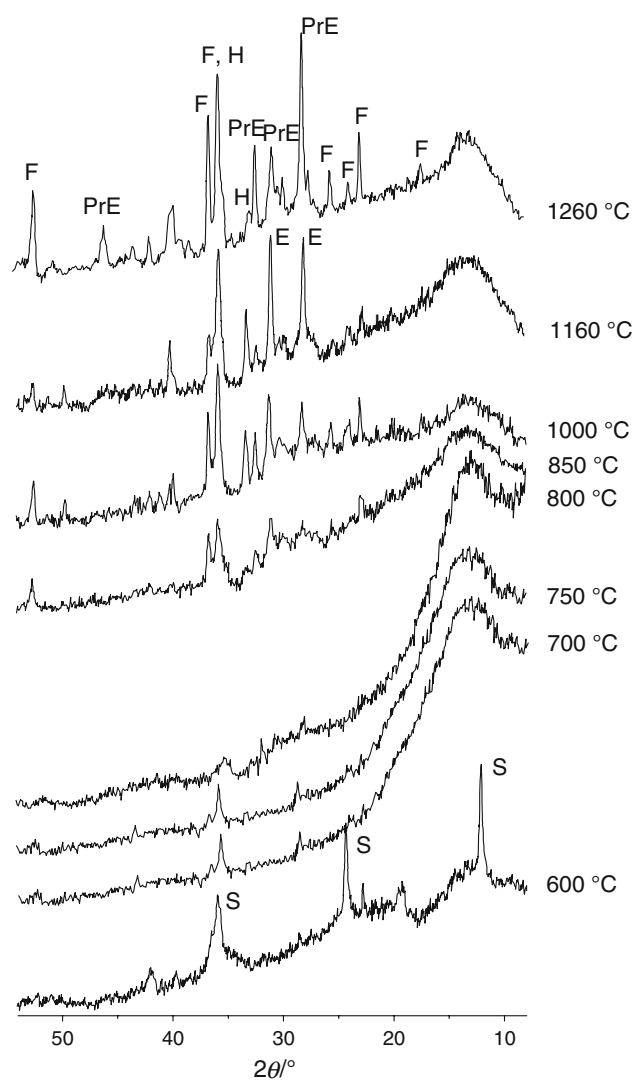


**Fig. 8** The XRPD patterns of the residue remained after acid processing of the NI-1 sample heat treated at the above mentioned temperatures. *S* serpentine, *F* forsterite, *E* enstatite, *PrE* protoenstatite, *H* hematite

the SSL. In this case, the removal of hydroxyl water and the breaking of Si–O bonds in siloxane bridges promote the release of such amount of orthosilicate anions that is enough for the progress of their spontaneous local arrangement along with $Mg^{2+}$ cations and results in the formation of the isolated nanocrystals of forsterite. On the one hand, these crystals easily react with acid. On the other hand, they are so large that their migration and transposition are impeded up to 850 °C. For this temperature, only the energy input promotes the migration and transposition of nano-sized forsterite crystals into larger and more completely formed ones.

The samples of SJ-1 and SJ-2 are characterized by the more uniform distribution of primary hydrated *ortho-* and *meta*-silicate anions in the SSL. As a result, the formation

of forsterite units is impeded because during the SSL destruction most of these anions remain in unbound state. Consequently, the migration of orthosilicate anions toward the forsterite nucleus formation followed by their further coalescence occurs at lower temperatures. It is remarkable that these forsterite units are more resistant to the acid influence (Fig. 5).

The comparatively lower endothermic peak intensity with minimum of 738 °C observable for the sample of NI-1 on the DTA curve (Fig. 4c) originates from (i) the overlap of two endothermic effects caused by the processes of the serpentinite decomposition, and (ii) from the removal of

The observable interdependence between the yields of soluble silicic acids and the amount of the removed hydroxyl water on heating (Figs. 2, 3) indicates that the SSL destruction directly depends on the separation of (OH) groups bonded with magnesium ions of the octahedral layer (see infra schema) [36]. It can be said that the SSL formed under hydrothermal conditions is stable in close unity with the (OH) groups of the "brucite" layer $Mg(OH)_2$. It follows that first of all the breaking of Si–O–Si bridges is caused by the imbalance of force field between the SSL and "brucite" layer stimulated by dehydroxylation on heating.
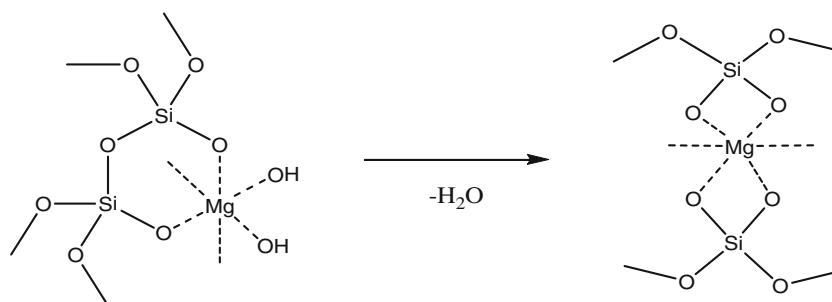


hydroxyl water, with the exothermic effect of the forsterite nanocrystals formation (Fig. 6). Therefore, the less intense exothermic effect with maximum of 841 °C on the DTA curve of the NI-1 sample can be referred to the processes of forsterite enlargement and recrystallization. As for the endothermic effects with minimum of 686 and 702 °C observed on the SJ-1 and SJ-2 samples curves, respectively, they are mainly caused by the processes of the serpentinite decomposition and the hydroxyl water removal, and the exothermic effects of more intensity with maxima of 820 and 842 °C for the samples of SJ-1 and SJ-2, respectively are mainly caused by the forsterite and partly enstatite formation (Card No 86–0433) (Fig. 5). It is quite logical to conclude that the source of these exothermic effects of the SJ-1 and SJ-2 samples can be also the overlap of the processes of forsterite enlargement and recrystallization.

To our belief, the enstatite formation at these temperatures (about 850 °C) occurs via the migration and rearrangement of *meta*-silicate anions originally involved in the SSL formation as they are released from surrounding $(SiO_4)^{4-}$ anions primarily existing in the SSL. However, the enstatite formed at these temperatures is incompletely formed and partly reacts with deluted acid. No wonder that on the diffraction patterns of the annealed samples and the residue, there are some differences in the intensities of the enstatite reflections (Figs. 5, 6, 7, 8).

In other words, as olivine and enstatite minerals dissolved from dunite, peridotite, and pyroxenite under hydrothermal conditions, the concentration of hydrated $(SiO_4)^{4-}$ and $[(SiO_3)^{2-}]_n$ anions and $Mg^{2+}$ ($Fe^{2+}$) cations in the serpentine-forming solution increased, thereby promoting the polycondensation of these anions in the form of the pseudohexagonal silicate layer. This process was accompanied by parallel forming of the cementing "brucite" layer.

Naturally, the stability of this system must mainly depend on (OH) groups. So, as experimental data have shown, on heating the separation of (OH) groups and the hydroxyl water removal are indispensably accompanied by the SSL partition. Thus, the SSL radically differs from the kaolinite silicate layer. Actually, the formation of Si–O–Si bridges in kaolinite proceeds in a different way. Hence, dehydroxylation does not have any influence on the stability of the kaolinite silicate lattice (or the stability of the kaolinite silicate lattice does not depend upon dehydroxylation) [35, 39, 40].

As stated above, the beginning of the silicate layer decomposition at comparatively low temperatures is caused by the existence of weak unsaturated Si–O(Si) bonds of siloxane bridges, which arise during the silicate layer formation at the temperatures of 500–400 °C and lower. Therefore, the separation of (OH) groups from "brucite" layer promotes the breaking of unsaturated bonds

of siloxane bridges, i.e., the silicate anions that originally participated in the SSL formation are reconstituted (regenerated). Actually, the number of primary hydrated $(SiO_4)^{4-}$ anions participating in the SSL formation is proportional to the number of siloxane bridges built with unsaturated Si–O bonds (it should be recalled that in the meta-silicate chains the Si–O–Si bridges were formed in magma, so their Si–O bonds are saturated and thus strong).

Assuming that the silicate layer was formed only by hydrated $(SiO_4)^{4-}$ anions, we can conclude that all the Si–O–Si bridges would be built with unsaturated Si–O bonds and the brucite layer of this type of the silicate layer would comprise the maximum allowed number of bonding hydroxyl groups in order to keep the system balance in whole. However, does it mean that if the SSL was exclusively formed by $(SiO_4)^{4-}$ anions, all those anions would be completely regenerated? This question can be answered on the basis of the following consideration. If the SSL is exclusively formed by $(SiO_4)^{4-}$ anions and its decomposition is not accompanied by any incidental processes, the following simplified version of the SSL destruction can be proposed:

$$Mg_6[Si_4O_{10}](OH)_8 \rightarrow 6Mg^{2+} + 3(SiO_4)^{4-} + SiO_2 + 4H_2O$$
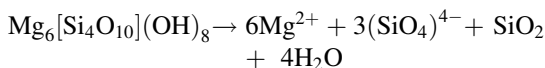
In other words, if MgO is completely recovered from serpentinites via thermo acid processing, the yields of $SiO_2$ must reach the maximum: 75 % in the form of soluble silicic acids and 25 % in the form of silica residue.

According to the data of chemical analysis the maximum yields of magnesium compounds are observed for the samples heated up to 750 °C (Fig. 3). However, unlike the NI-1 sample, the high yields of magnesium compounds are already observed for the specimens of SJ-1 and SJ-2 calcinated at the temperature of 600 °C. It means that if the silicate layer of serpentinous rocks is built with more evenly distributed ortho- and meta-silicate anions, the global amorphization of serpentinite crystalline structure occurs at comparatively low temperatures.

As stated above, the enstatite formation proceeds through the migration and reorientation of meta-silicate anions those originally moved into the serpentine-forming solution from dunite, pyroxenite, and peridotite, and were involved in the SSL formation. This process is in progress up to the temperature of about 1,000 °C. At higher temperatures, the enstatite formation can be caused by the rearrangement of released orthosilicate anions into meta-silicate ones. Therefore, the intensity of enstatite reflections up to the temperature of 1,000 °C indirectly indicates the ration of primary ortho- and meta-silicate anions participating in the SSL formation. The XRPD graphs show that for the samples of SJ-1, SJ-2, and NI-1, which are serpentinites formed from peridotites, the content of meta-silicate anions that participated in the SSL formation was low. This fact is also corroborated by the yields of soluble silicic acids (Fig. 3). Subsequent heating of the system (up to 1,160 °C and higher) results in the forsterite recrystallization and the transformation of esntatite into protoenstatite (Card No 85–2494).

## Conclusions

Via the above approach to the acid processing of dehydrated serpentines, it has been evidenced that the influence of heat treatment on the SSL are twofold. On the one hand, the process of dehydroxylation stimulates the SSL decomposition, resulting in the partition of the SSL into silicate anions of different complexities; and the number of splitting Si–O bonds in the siloxane bridges directly depends on the amount of hydroxyl water releasing on heating. On the other hand, the extent of the SSL decomposition does not depend upon the serpentines crystalline structure (chrisotile, lizardite, and antigorite) and is conditioned by particularities of the SSL structural organization. In this connection, it has been discovered two factors: (a) the different allocation and (b) the proportion of hydrated ortho- and meta-silicate anions originally involved in the process of the SSL formation, which govern the mechanism of temperature-induced decomposition of the serpentine silicate structure, including dehydroxylation, forsterite, and enstatite formation. These two factors (a) and (b) account for the stability of dehydroxylated phase, the extent of the SSL decomposition, and the temperature of forsterite and enstatite formation.

It should be emphasized that the stable dehydroxylated phases and the maximal decomposition extent of the SSL, resulting in the highest yields of soluble silicic acids and magnesium-containing compounds recovered via the acid processing, as well as high temperatures of forsterite formation ($\sim 800$ °C) are inherent in serpentinites (particularly, lizardites) with more even distribution of the considered anions in the SSL.

So, some differences observable for serpentines upon heating and various yields of soluble silicic acids recovered via the acid processing of amorphized masses of these minerals are caused by the peculiarities of the SSL organization rather than their crystalline variety.

These studies are of great value for the perception of the SSL formation mechanism and can be of considerable use in different branches of industry connected with serpentinites processing.

# References

1. Zulumyan NO, Isaakyan AR, Oganesyan ZG. A new promising method for processing of serpentinites. Russ J Appl Chem. 2007;. doi:10.1134/S1070427207060353.

2. Velinskii VV, Gusev GM. Production of extra pure silica from serpentinites. J Min Sci. 2002;38(4):402–4.

3. Teir S, Revitzer H, Eloneva S, et al. Dissolution of natural serpentinite in mineral and organic acids. Int J Min Process. 2007;. doi:10.1016/j.minpro.2007.04.001.

4. Gladikova LA, Teterin VV, Freidlina RG. Production of magnesium oxide from solutions formed by acid processing of serpentinite. Russ J Appl Chem. 2008;. doi:10.1134/S1070427208050339.

5. Fedoročková A, Hreus M, Raschman P, Sučik G. Dissolution of magnesium from calcined serpentinite in hydrochloric acid. Min Eng. 2012;32:1–4.

6. Torosyan AR, Zulumyan NH, Hovhannisyan ZH, Ghazaryan SE. The influence of mechanical processing on the process of Thermal Reduction of $SiO_2$ by Al Powder. In: Schlesinger ME, editor. EPD Congress 2005: Extraction & Processing Division. Salt Lake: TMS Extraction & Processing Division (EPD); 2005. p. 779–785.

7. Zulumyan NH, Isahakyan AR, Torosyan AR, Hovhannisyan ZH. The influence of mechanical activation on the process of thermal reduction of silica by magnesium powder. In: Luo AA, Neelameggham NR, Beals RS, editors. Magnesium Technology 2006 (The Minerals, Metals & Materials Society). TMS; 2006. p. 351–355.

8. Ball MC, Taylor HFW. Dehydration of chrysotile in air and under hydrothermal conditions. Miner Mag. 1963;33:467–82.

9. Brindley GW, Hayami R. Kinetics and mechanism of dehydration and recrystallization of serpentine. Clays Clay Miner. 1964;12:4–35.

10. Weber JN, Greer RT. Dehydration of serpentine: heat of reaction and reaction kinetics at $PH_2O = 1$ atm. Am Miner. 1965;50(3–4):450–64.

11. Naumann AW, Dresher WH. The influence of sample texture on chrysotile dehydroxylation. Am Miner. 1966;51:1200–11.

12. Brindley GW, Narahari Achar BN, Sharp JH. Kinetics and mechanism of dehydroxylation processes: ii. Temperature and vapor pressure dependence of dehydroxylation of serpentine. Am Miner. 1967;52:1697–705.

13. Cattaneo A, Gualtieri AF, Artioli G. Dehydroxylation of chrysotile asbestos with temperature by in situ XRPD. Phys Chem Miner. 2003;30:177–83.

14. Zaremba T, Krząkała A, Piotrowski J, et al. Study on the thermal decomposition of chrysotile asbestos. J Therm Anal Calorim. 2010;101:479–85.

15. Kusiorowski R, Zaremba T, Piotrowski J, Adamek J. Thermal decomposition of different types of asbestos. J Therm Anal Calorim. 2012;. doi:10.1007/s10973-012-2222-9.

16. Zaremba T, Piotrowski J, Gerle A. Thermal decomposition of asbestos-containing materials. J Therm Anal Calorim. 2013;. doi:10.1007/s10973-013-3038-y.

17. Trittschack R, Grobéty B. Dehydroxylation kinetics of lizardite. Eur J Miner. 2012;. doi:10.1127/0935-1221/2012/0024-2169.

18. Gualtieri AF, Giacobbe C, Viti C. The dehydroxylation of serpentine group minerals. Am Mineral. 2012;. doi:10.2138/am.2012.3952.

19. Brindley GW, Zussman J. A structural study of the thermal transformation of serpentine minerals to forsterite. Am Mineral. 1957;42:461–74.

20. Campbell FE, Roeder P. The stability of olivine and pyroxene in the Ni–Mg–Si–O system. Am Mineral. 1968;53:257–68.

21. Springer G. Compositional and structural variations in garnierites. Can Mineral. 1974;12:381–8.

22. Kononov ME, Protsyuk AP, Polyakov KI. Changes in olivine during heating in air. Refract Ind Ceram. 1993;. doi:10.1007/BF01283132.

23. MacKenzie KJD, Meinhold RH. Thermal reactions of chrysotile revisited; a 29 Si and 25 Mg MAS NMR study. Am Mineral. 1994;79(1–2):43–50.

24. Cheng TW, Ding YC, Chiu JP. A study of synthetic forsterite refractory materials using waste serpentine cutting. Miner Eng. 2002;. doi:10.1016/S0892-6875(02)00021-3.

25. Perrillat J-P, Daniel I, Koga KT, Reynard B, Cardon H, Crichton WA. Kinetics of antigorite dehydration: a real-time X-ray diffraction study. Earth Planet Sci Lett. 2005;. doi:10.1016/j.epsl.2005.06.006.

26. Hrsak D, Malina J, Hadzipasic AB. The decomposition of serpentine by thermal treatment. Mater Tehnol. 2005;39(6):225–7.

27. Gürtekin G, Albayrak M. Thermal reaction of antigorite: A XRD DTA–TG work. Miner Res Exp Bull. 2006;133:41–9.

28. Hrsak D, Sucik G, Lazik L. The thermophysical properties of serpentinite. Metal. 2008;47(1):29–31.

29. Viti C. Serpentine minerals discrimination by thermal analysis. Am Mineral. 2010;. doi:10.2138/am.2010.3366.

30. Bunjaku A, Kekkonen M, Holappa L. Phenomena in thermal treatment of lateritic nickel ores up to 1300 °C. In: The Twelfth International Ferroalloys Congress. Helsinki. 2010; June 6–9. p. 641–652.

31. Zulumyan N, Papakhchyan L, Isahakyan A, Beglaryan H, Terzyan A. Study of mechanical impact on the crystal lattice of serpentines. Geochem Int. 2011;. doi:10.1134/S0016702911090084.

32. Zulumyan NH, Papakhchyan LR, Terzyan AM, Beglaryan HA, Isahakyan AR. Structural features of the silicate networks of serpentines. Theor Found Chem Eng. 2013;. doi:10.1134/S0040579512040215.

33. Zulumyan NO, Isaakyan AR, Pirumyan PA, Beglaryan AA. The structural characteristics of amorphous silicas. Russ J Phys Chem A. 2010;. doi:10.1134/S003602441004031X.

34. Isahakyan AR, Beglaryan HA, Pirumyan PA, Papakhchyan LR, Zulumyan NH. An IR spectroscopic study of amorphous silicas. Russ J Phys Chem A. 2011;. doi:10.1134/S0036024410121015.

35. Zulumyan NH, Papakhchyan LR, Isahakyan AR, Beglaryan HA, Aloyan SG. Effect of mechanical treatment on the silicate lattice of kaolinite. Russ J Phys Chem A. 2012;. doi:10.1134/S003602441212028X.

36. Deer W, Howie R, Zussman J. Rock-forming minerals. Sheet silicates, vol. 3. London: Longmans; 1962.

37. Coleman RG. New idria serpentinite: a land management dilemma. Environ Eng Geosci. 1996;2(1):9–22.

38. Coleman RG. Prospecting for ophiolites along the California continental margin. Spec Pap-Geol Soc Am. 2000;349:351–64.

39. Richardson H. Phase changes which occur on heating kaolin clays. The x-ray identification and crystal structures of clay minerals. In: Brown G, editor. London: Mineral Soc.; 1972. p. 132–142.

40. Koç S, Toplan N, Yildiz K, Toplan HÖ. Effects of mechanical activation on the non-isothermal kinetics of mullite formation from kaolinite. J Therm Anal Calorim. 2011;103(3):791–6.